FEBS Letters 580 (2006) 4097–4104

Cell expression of a four extra octarepeat mutated PrP^C modifies cell structure and cell cycle regulation

Sergio F. Martín, María E. Herva, Juan-Carlos Espinosa, Beatriz Parra, Joaquín Castilla, Alejandro Brun, Juan M. Torres*

Centro de Investigación en Sanidad (CISA-INIA), Ctra. de Algete a El Casar, km. 8.100, 28130 Valdeolmos, Madrid, Spain

Received 4 May 2006; revised 19 June 2006; accepted 20 June 2006

Available online 30 June 2006

Edited by Jesus Avila

Abstract RK13 cell lines generated to express bovine PrP^C with a four extra octarepeat insertional mutation (Bo-10ORPrP^C) show partially insoluble PrP^C and lower rates of cell growth when compared to either the same cells expressing wild type Bo-6ORPrP^C or the original RK13 cell line. The expression of Bo-10ORPrP^C in cell cultures was also associated with changes in cell size and reorganization of the actin cytoskeleton. This last process was reversed by *Clostridium difficile* toxin-B, a specific inhibitor of small GTPase proteins. Further, in clones expressing Bo-10ORPrP^C, increased proportions of cells at cell cycle stage G2/M were observed. Proteasome inhibitors caused a further expansion of G2/M-stage cells that was more marked in cell lines expressing Bo-10ORPrP^C than those expressing Bo-6ORPrP^C, while this effect was minimal or null in the original RK13 cell line. Hence, the presence of Bo-10ORPrP^C in RK13 cells promotes cell cycle arrest at G2/M, and the effect is amplified by proteasome inhibition. These findings suggest a role for PrP^C in cell morphology and cell cycle regulation, and open new avenues for understanding the mechanisms underlying PrP mutation-associated diseases.

Keywords: Prion; PrP^C; Cell cycle; Actin cytoskeleton; Apoptosis; Small GTPase

1. Introduction

Prion diseases or transmissible spongiform encephalopathies are neurodegenerative disorders characterized by extensive neuronal apoptosis and a build up of PrP^{Sc}, a misfolded form of the cellular prion protein (PrP^C) [1–4]. Prion diseases such as scrapie in sheep, bovine spongiform encephalopathy (BSE) in cattle, and Creutzfeldt–Jakob disease in man, may be of an infectious origin. Inherited prion diseases has been only described in humans and have been associated with both point mutations and an increased number of octarepeats in the PrP^C open reading frame (ORF) [5–8]. The cellular mechanism by which mutations in the prion protein gene causes neurological dysfunction is unknown. It has been proposed that neuronal death can be triggered by accumulation of PrP in the cytosol due to impairment of proteasomal degradation of misfolded PrP molecules retrotranslocated from the endoplasmic reticulum [9].

In previous work, transgenic (Tg) mouse models expressing PrP^C with four or nine octapeptide insertional mutations showed a prion-like disease characterized by gliosis, and apoptotic loss of cerebellar granule cells [10,11] analogous to the disease observed in patients with a four extra repeat mutation in the PrP^C gene [6]. Furthermore, it has been shown that PrP^C with insertional mutations acquires special properties that may be reminiscent from PrP^{Sc}: ligand-binding, oxidative attack susceptibility, detergent insolubility, increased protease resistance, and aggregation capacity [5,12–15]. These properties suggest that insertional mutations confers neurotoxic properties (but not infectious) in PrP as showed by the neurodegerative phenotype associated with these mutations [10,11,16]. It is thus clear that a greater understanding of PrP^C structure and the effects of adding octarepeats to its coding region are required.

The present study was designed to explore prion related disorders of inherited origin using an experimental cell model. For this purpose, we used an epithelial RK13 cell line with no detectable PrP^C expression to generate two different cell lines expressing the normal Bo-PrP^C (Bo-6ORPrP) or a mutated form containing four extra octapeptide repeats (Bo-10ORPrP). Bo-10ORPrP acquired different biochemical properties and modified the RK13 cell phenotype by disrupting the reorganization of the actin cytoskeleton and normal cell cycle regulation. These findings open a new avenue for understanding the role of PrP^C in cellular homeostasis.

2. Materials and methods

2.1. Cell line and culture conditions

The rabbit kidney cell line RK-13 (WT), obtained from ATCC (CCL 37), was derived from kidney cells from a 5-week-old rabbit. These cells were cultured in Dulbecco's modified Eagle's minimum-essential medium (Grand Island Biological Company-Bethesda Research Laboratories (GIBCO-BRL), Bethesda, MD, USA) supplemented with 5% fetal bovine serum (Hyclone, Salt Lake City, UT, USA), 2 mM L-glutamine, 1% non-essential amino acids and 100 U/ml penicillin. Cell lines were cultured in a humidified atmosphere containing 5% CO_2 in air at 37 °C. Cell viability was determined by the trypan blue exclusion method.

*Corresponding author. Fax: +34 91 6202243.
E-mail address: jmtorres@inia.es (J.M. Torres).

Abbreviations: PrP^C, cellular prion protein; OR, octapeptide repeat; Bo-10ORPrP^C, bovine PrP^C with a four extra octarepeat insertional mutation; Bo-6ORPrP, normal Bo-PrP^C; ORF, open reading frame; Tg, transgenic

0014-5793/$32.00
doi:10.1016/j.febslet.2006.06.054

2.2. Plasmid constructs from bovine PrP and insertion mutants

The open reading frame (ORF) of the bovine PrP gene was obtained by PCR amplification from genomic bovine DNA using primers that create a *Not*I restriction enzyme site adjacent to the translation start codon (5′-GCGGCCGCATCATGGTGAAAAGCCACATAG-3′) and the stop site (5′-GCGGCCGCCTATCCTACTATGAGAAAA-ATG-3′). The 5′ primer also included Kozak sequences [17]. The PCR fragment was subcloned into a T-tailed vector and the insert was sequenced, confirming six copies of the octarepeat sequence and no changes in the amino acid sequence inferred from previously sequenced bovine PrP genes (GenBank accession number AF455119). The four extra octarepeats were introduced into the six-octarepeat bovine PrP gene as follows: 5′-CATGGAGGTGGCTGGGGCCA-GCCC-3′ and 5′-CATGGGGCTGGCCCCAGCCACCTC-3′ primers were used to obtain a tandem of four artificial octarepeats containing ends compatible with the *Nco*I restriction enzyme site. The PrP ORF was partially cut with the *Nco*I to avoid eliminating the native OR, and the tandem of four artificial octarepeats containing compatible extremes to *Nco*I was inserted. These plasmids were digested with *Not*I and inserted into the *Not*I site of pCMV plasmid to obtain the final plasmids designated as pCMVbo6ORPrP and pCMVbo10ORPrP.

2.3. Transfecting the RK13 cells

RK13 cells were cultured on 6-well sterile plastic trays (Nunc). At 70% confluence, cells were transfected with the above mentioned endonuclease digested constructs and cotransfected with pKneo plasmid (Stratagene). After selection with geneticin (G418; 500 μg/μl), cells were subcloned and analyzed by Western blotting and indirect immunofluorescence. Two clones showing different levels of PrP expression were selected for each construct: two clones expressing the normal Bo-6ORPrP^C (clones 8 and 2.4) and two clones expressing the mutant Bo-10ORPrP^C (clones 3.1 and 4.1).

2.4. Detecting PrP by Western blotting

Cells were seeded (30000 cells/well) in 6-well sterile plastic trays. Upon confluence, cells were harvested with PBS 0,05% EDTA and after $5000 \times g$ centrifugation 5 min, the pellet was resuspended in potassium buffer 20 mM. The protein concentrations of cell extracts were determined by the BCA protein assay (Pierce). 20 μg of protein were used in a 90 μl final volume. 10 μl of 10% SDS was added to every sample and boiled during 10 min. Then, four volumes of deglycosylation buffer (20 mM potassium buffer, 30 mM EDTA, 0,8% NP-40, 1.2% Triton X-100, 1.2% β-mercaptoethanol) were added and divided in two tubes. One of the two tubes was treated with 5 U of *N*-glycosidase F (NGF) (Roche). After incubation over night, 4 vol. of cold methanol were added and samples were incubated 2 h at −70 °C. Finally, they were centrifuged during 30 min at $20000 \times g$ and the pellet was resuspended in SDS sample loading buffer and then boiled for 10 min before loading on an SDS/12% polyacrylamide gel. Anti-PrP mAbs 6H4 (Prionics) or 2A11 [18] were used at 1/5000 and 1/1000 dilutions, respectively for immunoblotting. Immunocomplexes were detected using horseradish peroxidase conjugated anti-mouse IgG (Sigma Chemical Co.). Immunoblots were developed with enhanced chemiluminescence ECL (Amersham).

2.5. Detecting PrP by flow cytometry

Cells were harvested with 0.5 M EDTA in PBS, washed twice in PBS and blocked in 1× Perm Wash buffer (Pharmingen). To obtain permeabilized intact cells, cells were incubated with 2% formaldehyde in PBS for 20 minutes at 4 °C and washed three times in 1× Perm Wash buffer. All cellular samples, permeabilized and non permeabilized cells, were then incubated for 60 min at 4 °C with the 2A11 anti-PrP mAb (1:2000), and then with Alexa Fluor 488 goat anti-mouse IgG (A-11029, Molecular Probes) (1:200). Finally, the cells were examined by FACScan (Becton Dickinson, USA) at excitation and emission wavelengths of 475 and 520 nm, respectively. In each analysis, 5000 cells were examined.

2.6. Triton/Doc insolubility and proteinase-K sensitivity assay

Detergent insolubility of Bo-6ORPrP^C and Bo-10ORPrP^C expressed in RK13 cell lines was tested following the procedure previously described [19] with minor modifications. Confluent cells (5×10^6 cells/sample) were lysed in Triton/Doc buffer (0.5% TX-100, 0.5% Na-deoxycholate, 150 mM NaCl, and 100 mM Tris, pH 7.5) for 20 min at 4 °C and PrP^C was quantified in each case by Western blot. Nine volumes of the same buffer (ice-cold) were added to the whole cell extracts and equivalent amounts of PrP^C were centrifuged ($1000 \times$ g, 10 min, 4 °C). The supernatants were centrifuged at $25000 \times g$ for 60 min at 4 °C (Hettich zentrifugen, Germany). PrP^C was recovered in the supernatants by methanol precipitation, while the pelleted fractions were resuspended in the same buffer (containing 0.5% TX-100, 0.5% Na-deoxycholate). Insoluble PrP^C fractions were treated with 2 μg/ml of proteinase K (PK) for 1 h at 37 °C. All fractions whether PK treated or not were analyzed by SDS–PAGE/Western blotting using 2A11 anti-PrP mAb as described above.

2.7. Total cell counts and viable cell numbers

Total cell counts were performed using a haemocytometer and viable cells were counted after trypan blue exclusion (T 8154, Sigma). An equal volume of 2× trypan blue buffer was added to all samples (10 μg total protein per sample) and non-viable and viable cells quantified in each one by observation under the light microscope.

2.8. Histochemical detection of intracellular α-actin filaments

Cells were grown on sterile glass coverslips. After washing twice in PBS, the cells were incubated in 70% methanol in water for at least 1 h at 4 °C. This fixative was removed and cells were washed twice in PBS. Subsequently, the cells were incubated for 30 min with an anti-α-actin mAb (MS-1296, LabVision corporation) (1:2000) followed by the Alexa Fluor 488 goat anti-mouse IgG (A-11029, Molecular Probes) (1:200). Finally, the cells were examined under a fluorescence microscope (Nikon Phase Contrast-2 ELWD 0.3) at excitation and emission wavelengths of 475 and 520 nm, respectively, and images captured and analysed using a digital camera (Hamamatsu ORCA-ER digital camera C4742-95).

2.9. Detecting actin and/or nuclear DNA by flow cytometry

Propidium iodide (P-4170, Sigma), like ethidium iodide, intercalates with the nucleic acid helix and produces an increase in fluorescence detectable using excitation and emission wavelengths of 475 and 615 nm, respectively. The Alexa-488 conjugated antibody against α-actin is nevertheless fluorescent per se using excitation and emission wavelengths of 475 and 525 nm, respectively. Both indicators could be used together in the same sample. To determine α-actin levels or/and nuclear DNA contents, cells were trypsinized and then neutralized in DMEM medium. After washing twice in PBS, the cells were fixed using 70% methanol at 4 °C for at least an hour. After incubation (30 min at 4 °C) with an anti-α-actin mAb (1:2000), the cells were incubated with the Alexa Fluor 488 goat anti-mouse IgG (A-11029, Molecular Probes) (1:200). Finally, 5 rmug/ml RNAse and 10 μg/ml propidium iodide were added at room temperature for at least for 30 min. These samples were measured using a FACScan flow cytometer (Becton Dickinson, San Jose, CA) with excitation and emission wavelengths set at 475 and 525/615 nm, respectively. In each analysis, 5000 events were recorded.

2.10. Proteasome inhibition with MG132

For proteasome inhibition experiments, cells were seeded at 30000 cells/well in 6 well plates, three wells per cell line. Twenty-four hours later cells were harvested and medium replaced with complete minimum essential medium containing 5 μM of MG132 and the cells incubated for 0, 12 or 24 h at 37 °C. After treatment, cells were stained with 10 μg/ml propidium iodide and 5 μg/ml RNase A at 37 °C in dark and their cell cycle stages determined by flow cytometry.

Proteasome activity was measured in all cell lines before the addition of any inhibitor using the Proteasome-Glo™ Cell-Based Assay (Promega) and analyzed with the LUMIstar Galaxy Luminometer (BMG).

3. Results

3.1. Expression of normal and mutated forms of bovine PrP^C in the RK13 cell line

A set of cell lines were obtained from the RK13 cell line, from which we selected groups of cell lines according to PrP^C

expression levels: two clones expressing Bo-6ORPrP^C (clones 8 and 2.4) and two clones expressing Bo-10ORPrP^C (clones 3.1 and 4.1). As shown in Fig. 1A, bovine PrP^C protein expression was examined in these cell lines by Western blotting using the 2A11 monoclonal antibody. The blots indicated higher expression levels in clones 2.4 and 3.1 than in clones 4.1 and 8. No PrP^C expression could be detected in the wild type RK13 cell line as previously described [20]. To verify the differences in molecular weight between the Bo-6ORPrP^C and Bo-10ORPrP^C proteins, PrP^C glycans were removed by endoglycosidase (PNGaseF) digestion. As expected, the proteins showed different relative mobilities (Fig. 1A).

3.2. Subcellular localization of Bo-6ORPrP^C and Bo-10ORPrP^C

The subcellular localizations of Bo-6ORPrP^C and Bo-10ORPrP^C expressed in RK13 cell lines were analyzed by flow cytometry in permeabilized and non-permeabilized cells using the PrP specific mAb 2A11 as described in Section 2. While no labelling was detected in the original RK13 cell line, all clones expressing either Bo-6ORPrP^C (clones 8 and 2.4) or Bo-10ORPrP^C (clones 3.1 and 4.1) showed intense labelling for PrP (Fig. 1B). No significant differences were observed when compared the ratio of cell surface PrP (non-permeabilized)/total PrP (permeabilized cell) in the different cell lines. These results indicate that both Bo-6ORPrP^C and Bo-10ORPrP^C protein expressed in RK13 have a similar cellular distribution. Both proteins showed a preferential intracellular location but also occur at the cell surface. This finding was confirmed by immunofluorescent microscopy (data not shown).

3.3. Biochemical properties of Bo-10ORPrP^C expressed in RK13 cell lines

In a previous study [11], we noted that Bo-10ORPrP^C expression in transgenic mice gave rise to a build up of an insoluble and partly proteinase K-resistant form of PrP^C in the brain. To establish whether RK13-derived Bo-10ORPrP^C

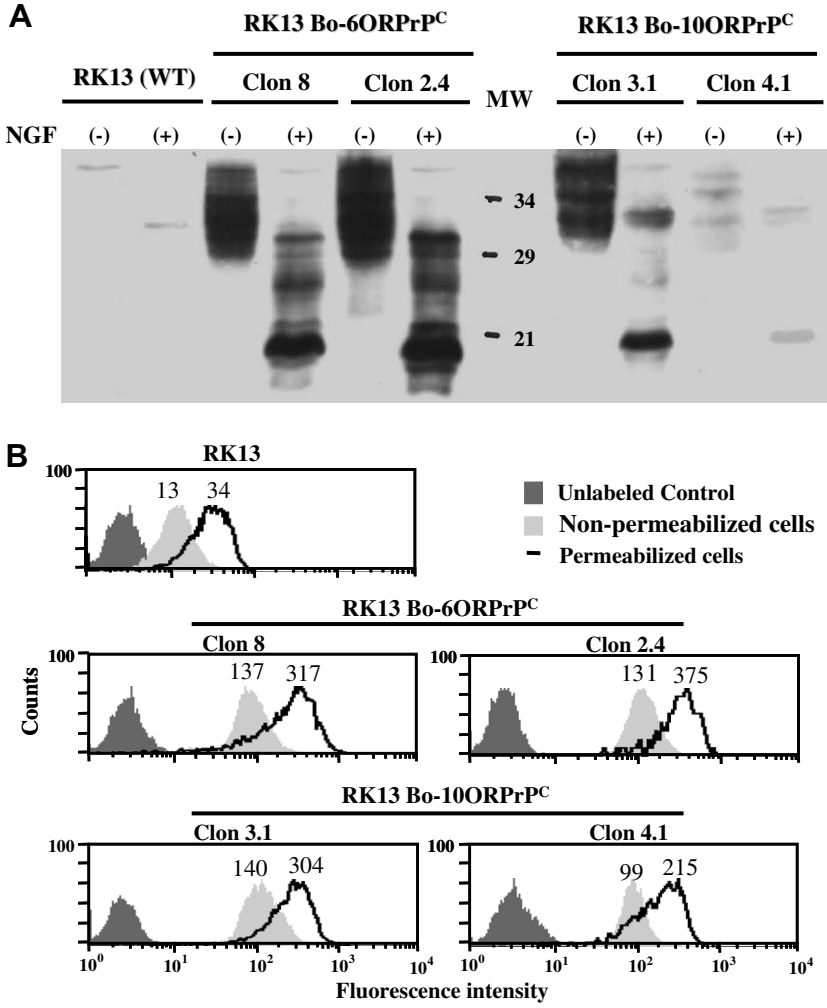

Fig. 1. Analysing the expression of wt Bo-6ORPrP^C and mutated Bo-10ORPrP^C in RK13 cell lines by Western blotting and FACs. (A) Cells lines were seeded at a density of 30 000 cells/well in 6-well sterile plastic trays. Upon confluence, cell lysates were treated or not treated with *N*-glycosilase F (NGF). All fraction, NGF-treated or not, were analysed by Western blotting using the anti-PrP^C mAb 2A11. Equivalent amounts of total protein were loaded on each lane. The data shown were obtained from one representative experiment out of three yielding identical results. The relative molecular mass (MW) appears in kilodaltons. (B) Flow cytometry analysis of permeabilized and non-permeabilizaed cells using the anti-PrP^C mAb 2A11. Histograms corresponding to PrP^C fluorescence distribution (*X*-axis: PrP^C fluorescence produced by Alexa 488, *Y*-axis: number of cells) observed in one representative experiment out of three producing similar results.

acquires insolubility and partial resistance to PK digestion, cell extracts were analysed as indicated in Section 2. No protease resistant PrP could be found in any cell line tested under the conditions used in this assay. However, Bo-10ORPrP^C protein was found to be partially insoluble in non-denaturing detergent extracts, while Bo-6ORPrP^C protein was only found in the soluble fraction (Fig. 2). These results are consistent with the properties of these same proteins expressed in transgenic mice [11].

3.4. RK13 cell lines expressing Bo-10ORPrP^C show an increased cell size but not a pro-apoptotic phenotype

In transgenic mouse models expressing PrP^C with four or nine octarepeat insertional mutations [10,11], the neuropathological changes produced are characterized by PrP deposition in different brain areas, gliosis, and loss of cerebellar granule cells. Thus, apoptotic cell death is a normal phenomenon in these transgenic mice. To establish whether Bo-10ORPrP^C could give rise to a pro-apoptotic phenotype upon expression in cell cultures, we subjected cells to different apoptotic stimuli (Supplemental figure 1A). It was found that hydrogen peroxide, tumour necrosis factor alpha, and serum deprivation induced similar mortality rates in all cell lines independently of the PrP^C expressed. Thus, none of these stimuli led to a PrP^C dependent pro-apoptotic phenotype.

In the search for phenotypic differences between cell lines expressing Bo-6ORPrP^C and Bo-10ORPrP^C, we then examined cellular senescence in the cultures. As shown in Supplemental figure 1B, no significant differences in the times to senescence were found among the cell lines, although lower absolute cell numbers were attained in Bo-10ORPrP^C-expressing cells than in Bo-6ORPrP^C-expressing cells or original RK13 cells (Supplemental figure 1A). To investigate these differences in the cell populations, cells were grown on culture plates and cellular morphology examined by staining for α-actin. As revealed in Fig. 3A, in clones 3.1 and 4.1 expressing Bo-10ORPrP^C, several larger cells appeared, which were absent from the wild type RK13 or Bo-6ORPrP^C-expressing cell lines (clones 8 and 2.4). This larger cell size observed among cells expressing Bo-10ORPrP^C appeared in normal growth conditions. However, after trypsin treatment of the cell culture monolayer, each cell line displayed similar cell morphology, both by light microscopy and flow cytometry (Fig. 3B). Thus, the cell size differences observed only appeared under adherence on culture plates but not after trypsin treatment.

To establish whether the altered cell morphology was a biological process directly related to the actin cytoskeleton, we also quantified the amount of actin filaments in each cell line by flow cytometry using anti-α-actin antibodies. Actin contents failed to vary significantly among the cell lines (Fig. 3B). Given these similar amounts of actin in Bo-10ORPrP^C – and Bo-6ORPrP^C-expressing cells as well as in the original RK13 cells, the larger cell sizes observed in the Bo-10ORPrP^C – producing clones could be related to the presence of cytoskeleton architecture regulators. However, we can not discard the possibility that the absence of cell size differences after trypsin treatment could be due to the low number of enlarged cells poorly represented in the pool of cells analyzed.

3.5. GTPase protein inhibitors recover the normal phenotype of Bo-10ORPrP-expressing cells

The small family of GTPases, Rho, Cdc42 and Rac1, comprises the most important regulators of the actin cytoskeleton, affecting cell shape and movement. In order to decipher if small GTPases could be regulating the increased cell size observed in the Bo-10ORPrP^C-expressing clones, we incubated cell monolayers with *Clostridium difficile* toxin-B. As shown in Fig. 4, the enlarged cell phenotype of the Bo-10ORPrP^C-expressing clones was reversed after incubation with the toxin. These small GTPase proteins therefore seem to play a role in increasing cell size in these cell lines. Interestingly, nuclei were larger in the Bo-10ORPrP^C-expressing clones than in the remaining cell lines. These observations suggest that Bo-10ORPrP^C-expressing clones have larger amounts of DNA, which is indicative of cell cycle dysregulation.

Clones expressing Bo-10ORPrP^C showed increased proportions of cells at the G2/M stage and this effect is amplified by proteasome inhibition. To explore whether the cell cycle was altered in the Bo-10ORPrP^C-expressing cells, DNA was stained with propidium iodide and subjected to flow cytometry analysis. An approximate 20% increase in the number of G2/M

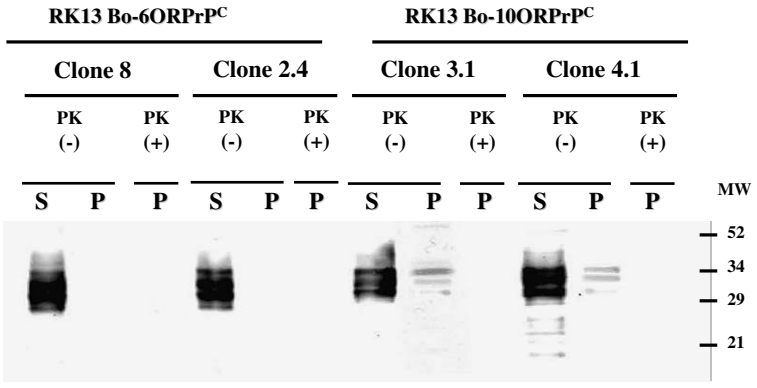

Fig. 2. Insolubility and proteinase-K sensitivity of wt Bo-6ORPrP^C and mutated Bo-10ORPrP^C expressed in RK13 cells. Soluble and insoluble PrP^C fractions from cell lysates in Triton/Doc buffer were obtained after centrifugation at 25000 × *g* for 60 min as described in Section 2. Insoluble PrP^C fractions were treated or not treated with 2 μg/ml of proteinase K (PK) for 1 h. All fraction, PK-treated or not, were analyzed by SDS–PAGE/Western blotting using the 2A11 anti-PrP mAb. The data shown were obtained from one representative experiment out of three producing identical results.

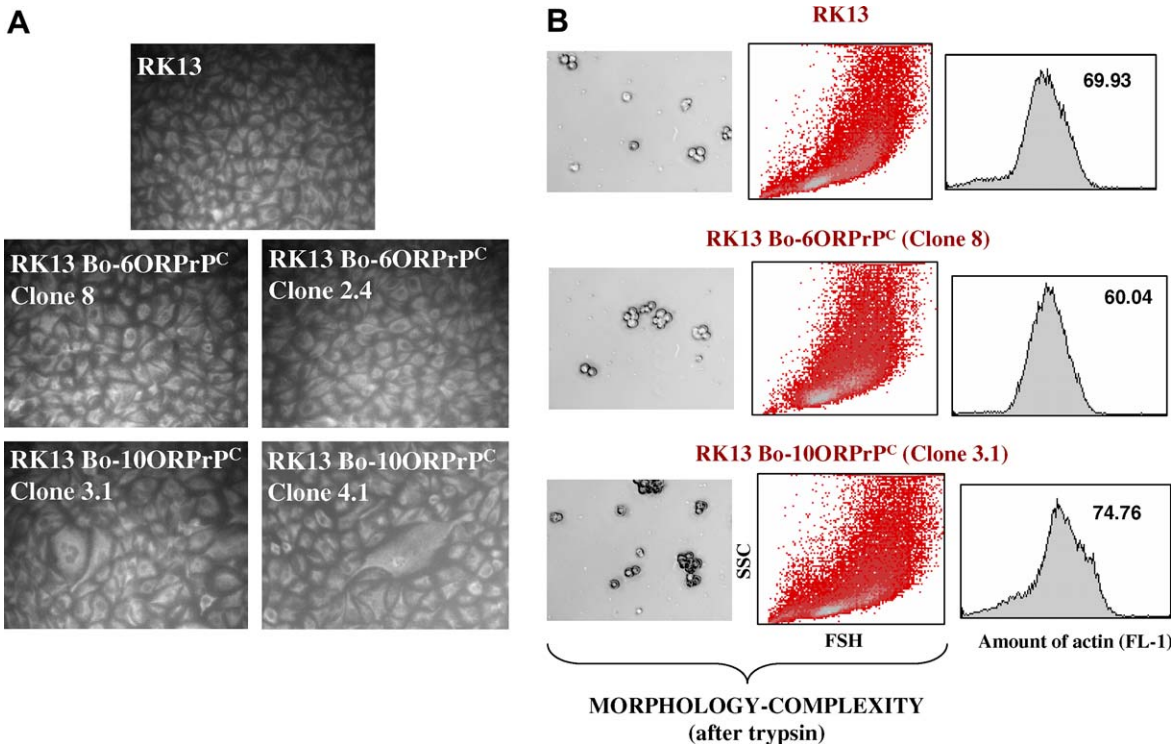

Fig. 3. Analysis of the morphology-complexity and amount of actin in RK13 cells expressing wt Bo-6ORPrP^C or mutated Bo-10ORPrP^C. (A) Cells lines were seeded (30000 cells/well) in 6-well sterile plastic trays. Upon confluence, the medium was replaced with serum-free minimum essential medium, and the cells incubated with the anti-actin mAb followed by the Alexa Fluor 488 goat anti-mouse IgG as described in Section 2. Each cell line was visualized and analyzed by fluorescence microscopy. Representative fields are shown at a magnification of 25×. Note the enlarged cells indicated by white arrows. (B) Cell lines were cultured as described above but upon confluence they were trypsinized and neutralized using medium. Morphology-complexity was assessed in each cell line by light microscopy (column 1) and flow cytometry (*X*-axis: FSH, *Y*-axis: SSC) (column 2). Representative light microscopy fields are shown at a magnification of 25×. Trypsinized cells were also used to evaluate the total actin amounts by flow cytometry (column 3) as described in Section 2. Histograms show the actin fluorescence distribution (*X*-axis: actin fluorescence by Alexa 488, *Y*-axis: number of cells) recorded in one representative experiment out of three.

cells was observed among the Bo-10ORPrP^C-expressing cells when compared to both Bo-6ORPrP^C-expressing and original RK13 cells (Fig. 5). This observation clearly points to cell cycle dysregulation.

It has been established that proteasome inhibition often accompanies protein aggregation in cells expressing PrP^C [21]. Thus, to determine if inhibition of the proteasome complex could enhance the expansion of G2/M cells expressing boPrP^C, cells were incubated with MG132. As represented in Fig. 6, the proteasome inhibitor induced slight G2/M cell expansion in the original RK13 cell line (4% and 9% after 12 and 24 h, respectively), and relatively increased G2/M cell expansion in the clones expressing Bo-6ORPrP^C (12–30%) and Bo-10ORPrP^C (40–55%). To determine whether this effect is caused by an inhibition of proteasomal activity by the expression of PrP^C or not we evaluated the proteasomal activity in the different cell lines before the addition of MG132 inhibitor. The results (supplemental figure 2) showed no significant differences in proteasomal activity between the different cell lines allowing us to exclude the possibility of an inhibition of proteasome activity by the expression of PrP^C. These data point to an expansion of G2/M cells promoted by proteasome blocking in all the cell lines (Fig. 6) and an amplified effect of proteasome inhibition in the presence of Bo-PrP^C protein, especially mutated PrP^C (Bo-10ORPrP).

4. Discussion

In this study, we used a cell model derived from the rabbit epithelial cell line RK13 expressing different forms of PrP^C: two clones expressing the wild type Bo-6ORPrP^C (clones 8 and 2.4) and two clones expressing the mutant Bo-10ORPrP^C (clones 3.1 and 4.1). The RK13 cell line was chosen on the grounds that: (i) these cells express no detectable protein levels of endogenous rabbit PrP^C, thus reducing the risk of interference with the activity of the transfected boPrP^C; and (ii) this cell line has already been used as an adequate background for the propagation of ovine prions [20]. In the present study, we observed that cells expressing the partially insoluble Bo-10ORPrP^C displayed an increased cell size and an expanded G_2/M-stage cell compartment. The data reported here provide insight into the possible mechanisms used by this peptide to promote disease.

In the RK13 cell line, the mutant Bo-10ORPrP^C protein was found to be partially insoluble, while the wild type Bo-6ORPrP^C protein was soluble. This finding correlates well with previous observations in transgenic mice expressing bovine PrP, in which the addition of four extra octapeptide repeats (Bo-10ORPrP) rendered a more insoluble PrP [11]. The reason for this increased insolubility remains to be established. It has been suggested that an increased number of OR causes enhanced aggregation of the mutant PrP protein in the

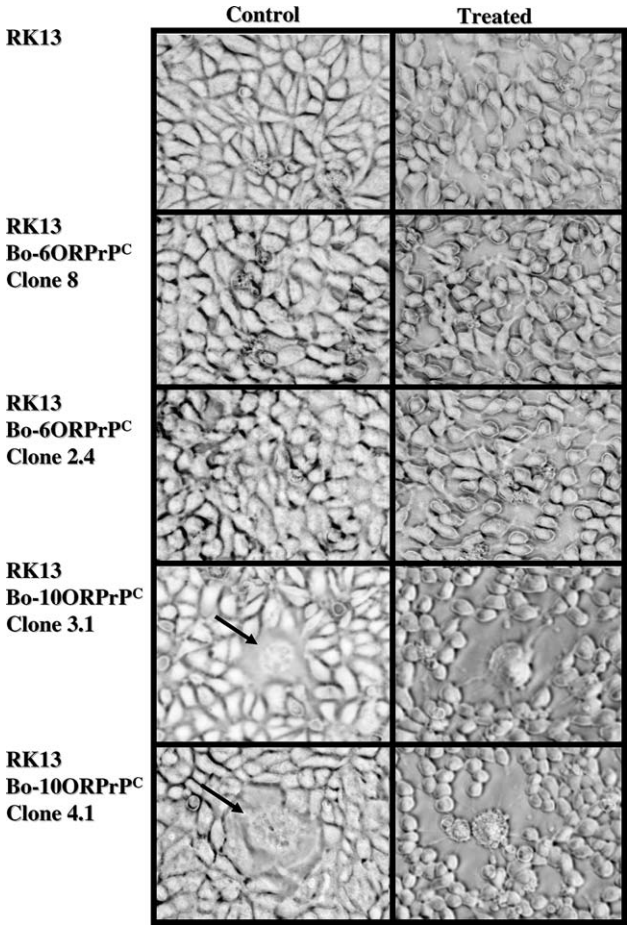

Fig. 4. Effect of the *Clostridium difficile* toxin-B on cell morphology. Cell lines were seeded (30 000 cells/well) in 6-well sterile plastic trays. Upon confluence, the medium was replaced with complete minimum essential medium containing 10 ng/ml of *Clostridium difficile* toxin-B and incubated for 3 h at 37 °C. After treatment, morphological changes in the RK13 cell lines were assessed by incubation with the anti-actin mAb followed by Alexa Fluor 488 goat anti-mouse IgG as described in Section 2 and light microscopy. The micrographs shown are representative of at least three independent experiments. Representative fields are shown at a magnification of 40×. Note the enlarged cells indicated by arrows.

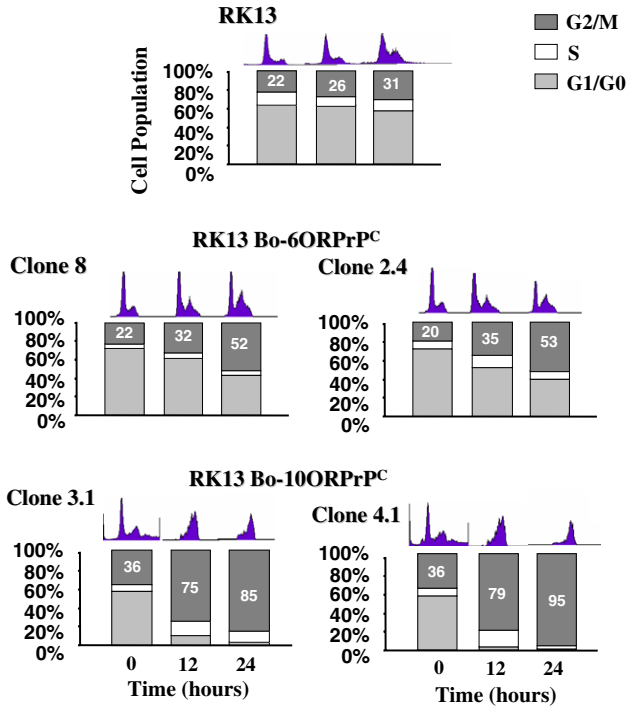

Fig. 6. Effects of proteasome inhibitors on the cell cycle stages of RK13 cells expressing wt Bo-6ORPrP^C or mutated Bo-10ORPrP^C. Cell lines were harvested when they reached 50% confluence. The medium was then replaced with complete minimum essential medium containing 5 μM of MG132 and the cells incubated for 0, 12 or 24 h at 37 °C. After treatment, cells were stained with 10 μg/ml propidium iodide and 5 μg/ml RNase A at 37 °C in dark and their cell cycle stages determined by flow cytometry as indicated for Fig. 5. Data are represented as histograms and bars to aid comprehension. The data shown are representative of at least three experiments.

hamster [5]. The repeat region of the prion protein has been proposed to act in itself as a site promoting PrP self-aggregation or aggregation between PrP and other cell factors [22,23]. It is also known that this protein is degraded through the actions of the proteasome [24]. Recent results have also indicated the role of the proteasome in degrading PrP, which

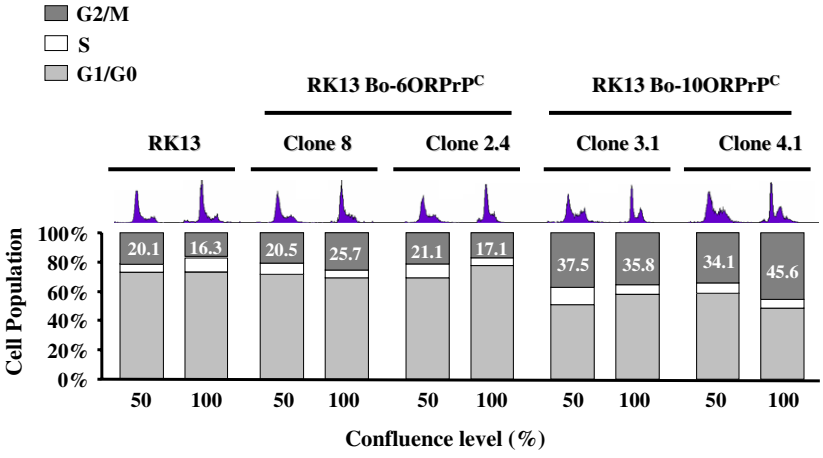

Fig. 5. Cell cycle stage of RK13 cells expressing wt Bo-6ORPrP^C or mutated Bo-10ORPrP^C. Each cell line was harvested upon reaching two levels of confluence (50% and 100%). The cells were then stained with 10 μg/ml propidium iodide and 5 μg/ml RNase A at 37 °C in the dark. Cell cycle stages were determined by establishing DNA amounts in each cell line by flow cytometry. Data are represented as histograms and bars to aid comprehension. The data shown are representative of at least three independent experiments.

may play a neurotoxic role in prion diseases [25]. In the present case, we propose that the build up of partially insoluble Bo-10ORPrP could be a consequence of impaired proteasomal activities increasing the life span of PrP in the cell. This would in turn favour the appearance of partially insoluble Bo-10ORPrP^C. Thus, the appearance of partially insoluble Bo-10ORPrP^C could hinder the elimination of PrP^C by the cell proteasome pathway.

The expansion of G_2/M-stage cells observed in all our cell lines was amplified by proteasome inhibition in a PrP^C dependent manner. Thus, the subset of G_2/M-stage cells in the native RK13 cell lines was unaffected by the proteasome inhibitor MG132. In contrast, G_2/M cell expansion was amplified in clones expressing the wild type Bo-6ORPrP^C and amplified further still in the clones expressing the mutant protein Bo-10ORPrP. These findings seem to suggest that the presence of modified PrP^C (Bo-10ORPrP) with a tendency towards aggregation seems to interfere with normal cell cycle regulation. To date, a role for PrP^C signalling in cell cycle control has not yet been reported. However, it is known that proteasome inhibitors induce an enrichment of G_2/M-stage cells [26]. Several authors have shown that the overexpression of both PrP^C and insertionally mutated PrP^C reduce the lifespan of animal models [11,26,27]. Moreover, an expansion of cells at G_2/M has been described in the rapid ageing disease progeria [28]. There are also reports that show a functional relationship between small GTPase proteins and PrP^C [29,30]. Hence, we could suggest an indirect relationship between G_2/M-stage cell expansion and PrP^C through small GTPase proteins. In porcine aortic endothelial cells, G_2/M cell expansion occurs when the constitutive active forms of Rac and Cdc42 are induced [31], promoting Ras over expression [32]. Collectively, our findings could support the idea that PrP may directly or indirectly affect the cell cycle by its arrest at the G_2/M stage.

In our study, cells expressing Bo-10ORPrP showed an increased size. Recovery of the normal phenotype by *Clostridium difficile* toxin-B (a specific inhibitor of small GTPase protein family members) suggests that the larger cell size could be caused by a normal GTPase-mediated action on the actin cytoskeleton. Nevertheless, the nucleus was relatively larger in these enlarged cells than normal. This suggests that the cell size increase occurs after cell cycle arrest at stage G_2/M. A relationship between the actin cytoskeleton and PrP^C has been indirectly reported by other authors, who indicate strong interaction between PrP^C and cytoskeleton components, such as β-actin and α-tubulin [33]. In a study focussing on PrP mRNA and smooth muscle α-actin mRNA in culture-activated stellate cells, strong correlation was revealed between both mRNAs [34]. In addition, a specific interaction has been noted between the cytoskeletal assembly protein sla1 and the prion-forming domain of the release factor Sup35 (eRF3) in *Saccharomyces cerevisiae* [35]. Finally, toxic PrP-derived peptide (PrP106-126) has been shown to bind to tubulin in cell-free assays and also to inhibit microtubulin formation mediated by tau [36]. Thus, we infer a possible functional relationship between PrP and actin cytoskeleton reorganization.

The increased cell size and the expanded G_2/M-stage cell compartment observed in cells expressing the mutant Bo-10ORPrP could constitute two overlapping phenomena. In adherence, the nucleus was relatively larger in these enlarged cells than normal; while an expansion of cells at G_2/M has been observed in solution. This suggests that the cell size increase occurs after cell cycle arrest at stage G_2/M, probably by a stop of mitosis in these mutant cells.

In addition, although it is generally accepted that neuronal loss is a cardinal feature of prion diseases, the role of apoptosis in this process has received limited attention. It is known that a synthetic peptide derived from the PrP^C sequence (PrP106–126) induces the apoptotic death of cultured neurons [37]. Several transgenic mice expressing mouse PrP with extra octapeptide insertional mutations have shown granule cell apoptosis, gliosis and loss of cerebellar granule cells [10,11]. Here, the expansion of G_2/M-stage cells in RK13 clones expressing Bo-10ORPrP was independent of a pro-apoptotic phenotype. However, it is known that some pro-apoptotic phenotype inducers including vincristine, β-catenin, nocodazole, paclitaxel, evodiamine, etc. render increased proportions of G_2/M-stage cells [38–45]. Thus, our findings in RK13 cells require confirmation using cultured nerve cells, in which apoptosis is known to be a feature of prion diseases.

In conclusion, the data presented indicate that a four extra repeat mutated PrP in RK13 cells induces changes in cell size and an expansion in G_2/M-stage cells, probably mediated by a small GTPase protein. Our results suggest that the presence of the modified PrP^C (Bo-10ORPrP), which has a tendency to aggregate, seems to interfere with the control of the normal cell cycle by causing arrest at the G2/M stage. In addition, the expansion of G_2/M-stage cells can be amplified by proteasome inhibition in a PrP^C dependent manner, suggesting a role for PrP^C in cell cycle regulation.

Acknowledgement: This work was supported by Grants RTA02-033 and UE CT2004-506579 FOOD.

Appendix A. Supplementary data

Supplementary data associated with this article can be found, in the online version, at doi:10.1016/j.febslet.2006.06.054.

References

[1] Prusiner, S.B. (1998) Prions. Proc. Natl. Acad. Sci. USA 95, 13363–13383.
[2] Stumpf, M.P. and Krakauer, D.C. (2000) Mapping the parameters of prion-induced neuropathology. Proc. Natl. Acad. Sci. USA 97, 10573–10577.
[3] Castilla, J., Hetz, C. and Soto, C. (2004) Molecular mechanisms of neurotoxicity of pathological prion protein. Curr. Mol. Med. 4, 397–403.
[4] Campana, V., Sarnataro, D. and Zurzolo, C. (2005) The highways and byways of prion protein trafficking. Trends Cell. Biol. 15, 102–111.
[5] Priola, S.A. and Chesebro, B. (1998) Abnormal properties of prion protein with insertional mutations in different cell types. J. Biol. Chem. 273, 11980–11985.
[6] Yanagihara, C., Yasuda, M., Maeda, K., Miyoshi, K. and Nishimura, Y. (2002) Rapidly progressive dementia syndrome associated with a novel four extra repeat mutation in the prion protein gene. J. Neurol. Neurosurg. Psychiat. 72, 788–791.
[7] Goldfarb, L.G., Brown, P., Cervenakova, L. and Gajdusek, D.C. (1994) Molecular genetic studies of Creutzfeldt–Jakob disease. Mol. Neurobiol. 8, 89–97.

[8] Capellari, S. et al. (1997) Familial prion disease with a novel 144-bp insertion in the prion protein gene in a Basque family. Neurology 49, 133–141.
[9] Ma, J. and Lindquist, S. (2002) Conversion of PrP to a self-perpetuating PrPSc-like conformation in the cytosol. Science 298, 1785–1788.
[10] Chiesa, R., Piccardo, P., Quaglio, E., Drisaldi, B., Si-Hoe, S.L., Takao, M., Ghetti, B. and Harris, D.A. (2003) Molecular distinction between pathogenic and infectious properties of the prion protein. J. Virol. 77, 7611–7622.
[11] Castilla, J., Gutiérrez-Adán, A., Brun, A., Pintado, B., Salguero, F.J., Parra, B., Díaz San Segundo, F., Ramírez, M.A., Rábano, A., Cano, M.J. and Torres, J.M. (2005) Transgenic mice expressing bovine PrP with a four extra repeat octapeptide insert mutation show a spontaneous, non-transmissible, neurodegenerative disease and an expedited course of BSE infection. FEBS Lett. 579, 6237–6246.
[12] Ivanova, L., Barmada, S., Kummer, T. and Harris, D.A. (2001) Mutant prion proteins are partially retained in the endoplasmic reticulum. J. Biol. Chem. 276, 42409–42421.
[13] Gauczynski, S., Krasemann, S., Bodemer, W. and Weiss, S. (2002) Recombinant human prion protein mutants huPrP D178N/M129 (FFI) and huPrP+9OR (fCJD) reveal proteinase K resistance. J. Cell Sci. 115, 4025–4036.
[14] Narwa, R. and Harris, D.A. (1999) Prion proteins carrying pathogenic mutations are resistant to phospholipase cleavage of their glycolipid anchors. Biochemistry 38, 8770–8777.
[15] Yin, S. et al. (2006) Prion proteins with insertion mutations have altered N-terminal conformation and increased ligand binding activity and are more susceptible to oxidative attack. J. Biol. Chem. 281, 10698–10705.
[16] Cochran, E.J. et al. (1996) Familial Creutzfeldt–Jakob disease with a five-repeat octapeptide insert mutation. Neurology 47, 727–733.
[17] Kozak, M. (1989) The scanning model for translation: an update. J. Cell Biol. 108, 229–241.
[18] Brun, A. et al. (2004) Proteinase K enhanced immunoreactivity of the prion protein-specific monoclonal antibody 2A11. Neurosci. Res. 48, 75–83.
[19] Lorenz, H., Windl, O. and Kretzschmar, H.A. (2002) Cellular phenotyping of secretory and nuclear prion proteins associated with inherited prion diseases. J. Biol. Chem. 277, 8508–8516.
[20] Vilette, D., Andreoletti, O., Archer, F., Madelaine, M.F., Vilotte, J.L., Lehmann, S. and Laude, H. (2001) Ex vivo propagation of infectious sheep scrapie agent in heterologous epithelial cells expressing ovine prion protein. Proc. Natl. Acad. Sci. USA 98, 4055–4059.
[21] Ma, J., Wollmann, R. and Lindquist, S. (2002) Neurotoxicity and neurodegeneration when PrP accumulates in the cytosol. Science 17, 17.
[22] Chiesa, R., Piccardo, P., Ghetti, B. and Harris, D.A. (1998) Neurological illness in transgenic mice expressing a prion protein with an insertional mutation. Neuron 21, 1339–1351.
[23] Jarrett, J.T. and Lansbury Jr., P.T. (1993) Seeding one-dimensional crystallization'' of amyloid: a pathogenic mechanism in Alzheimer's disease and scrapie? Cell 73, 1055–1058.
[24] Yedidia, Y., Horonchik, L., Tzaban, S., Yanai, A. and Taraboulos, A. (2001) Proteasomes and ubiquitin are involved in the turnover of the wild-type prion protein. Embo J. 20, 5383–5391.
[25] Harris, D.A. (2003) Trafficking, turnover and membrane topology of PrP. Br. Med. Bull. 66, 71–85.
[26] Ling, Y.-H., Liebes, L., Jiang, J.-D., Holland, J.F., Elliott, P.J., Adams, J., Muggia, F.M. and Perez-Soler, R. (2003) Mechanisms of proteasome inhibitor PS-341-induced G2-M-phase arrest and apoptosis in human non-small cell lung cancer cell lines. Clin. Cancer Res. 9, 1145–1154.
[27] Castilla, J. et al. (2003) Early detection of PrP(res) in BSE-infected bovine PrP transgenic mice. Arch. Virol. 148, 677–691.
[28] Ly, D.H., Lockhart, D.J., Lerner, R.A. and Schultz, P.G. (2000) Mitotic misregulation and human aging. Science 287, 2486–2492.
[29] Schneider, B., Mutel, V., Pietri, M., Ermonval, M., Mouillet-Richard, S. and Kellermann, O. (2003) NADPH oxidase and extracellular regulated kinases 1/2 are targets of prion protein signaling in neuronal and nonneuronal cells. Proc. Natl. Acad. Sci. USA 100, 13326–13331.
[30] Satoh, J., Kuroda, Y. and Katamine, S. (2000) Gene expression profile in prion protein-deficient fibroblasts in culture. Am. J. Pathol. 157, 59–68.
[31] Muris, D.F., Verschoor, T., Divecha, N. and Michalides, R.J. (2002) Constitutive active GTPases Rac and Cdc42 are associated with endoreplication in PAE cells. Eur. J. Cancer 38, 1775–1782.
[32] Spyridopoulos, I., Isner, J.M. and Losordo, D.W. (2002) Oncogenic ras induces premature senescence in endothelial cells: role of p21(Cip1/Waf1). Basic Res. Cardiol. 97, 117–124.
[33] Keshet, G.I., Bar-Peled, O., Yaffe, D., Nudel, U. and Gabizon, R. (2000) The cellular prion protein colocalizes with the dystroglycan complex in the brain. J. Neurochem. 75, 1889–1897.
[34] Ikeda, K., Kawada, N., Wang, Y.Q., Kadoya, H., Nakatani, K., Sato, M. and Kaneda, K. (1998) Expression of cellular prion protein in activated hepatic stellate cells. Am. J. Pathol. 153, 1695–1700.
[35] Bailleul, P.A., Newnam, G.P., Steenbergen, J.N. and Chernoff, Y.O. (1999) Genetic study of interactions between the cytoskeletal assembly protein sla1 and prion-forming domain of the release factor Sup35 (eRF3) in *Saccharomyces cerevisiae*. Genetics 153, 81–94.
[36] Brown, D.R. (2000) Altered toxicity of the prion protein peptide PrP106-126 carrying the Ala(117) → Val mutation. Biochem. J. 346 (Pt 3), 785–791.
[37] Forloni, G., Angeretti, N., Chiesa, R., Monzani, E., Salmona, M., Bugiani, O. and Tagliavini, F. (1993) Neurotoxicity of a prion protein fragment. Nature 362, 543–546.
[38] Huang, Y.C., Guh, J.H. and Teng, C.M. (2004) Induction of mitotic arrest and apoptosis by evodiamine in human leukemic T-lymphocytes. Life Sci. 75, 35–49.
[39] Mullan, P.B. et al. (2001) BRCA1 and GADD45 mediated G2/M cell cycle arrest in response to antimicrotubule agents. Oncogene 20, 6123–6131.
[40] Torres, K. and Horwitz, S.B. (1998) Mechanisms of Taxol-induced cell death are concentration dependent. Cancer Res. 58, 3620–3626.
[41] Halloran, P.J. and Fenton, R.G. (1998) Irreversible G2-M arrest and cytoskeletal reorganization induced by cytotoxic nucleoside analogues. Cancer Res. 58, 3855–3865.
[42] Kwan, R., Burnside, J., Kurosaki, T. and Cheng, G. (2001) MEKK1 is essential for DT40 cell apoptosis in response to microtubule disruption. Mol. Cell Biol. 21, 7183–7190.
[43] Moos, P.J. and Fitzpatrick, F.A. (1998) Taxane-mediated gene induction is independent of microtubule stabilization: induction of transcription regulators and enzymes that modulate inflammation and apoptosis. Proc. Natl. Acad. Sci. USA 95, 3896–3901.
[44] Sorger, P.K., Dobles, M., Tournebize, R. and Hyman, A.A. (1997) Coupling cell division and cell death to microtubule dynamics. Curr. Opin. Cell Biol. 9, 807–814.
[45] Li, F., Ambrosini, G., Chu, E.Y., Plescia, J., Tognin, S., Marchisio, P.C. and Altieri, D.C. (1998) Control of apoptosis and mitotic spindle checkpoint by survivin. Nature 396, 580–584.